Fractional diffusion interpretation of simulated single-file systems in microporous materials

Pierfranco Demontis and Giuseppe B. Suffritti*

Dipartimento di Chimica, Università di Sassari and Consorzio Interuniversitario Nazionale per la Scienza e Tecnologia dei Materiali (INSTM), Unità di ricerca di Sassari, Via Vienna, 2, I-07100 Sassari (Italy)

(Received 30 June 2006; published 15 November 2006)

The single-file diffusion of water in the straight channels of two different crystalline microporous aluminosilicates (zeolites bikitaite and Li-ABW) was studied by comparing the results of molecular dynamics computer simulations with the predictions of anomalous diffusion theory modeled by using fractional diffusion equations. At high coverage, the agreement is reasonably good, in particular for sufficiently large displacements and sufficiently long times. At low coverage, interesting phenomena appear in the simulation results, such as multimodal propagators, which could be interpreted on the basis of fractional Fokker-Planck equations. The results are discussed also in view of different theories that have been proposed to model the single-file diffusion process.

DOI: 10.1103/PhysRevE.74.051112 PACS number(s): 05.40.Jc, 05.60.−k

I. INTRODUCTION

Diffusion of particles, which occurs in channels so narrow that no mutual passage is possible, is usually referred to as single-file diffusion. Single-file diffusion is encountered in many systems, such as ion transport in biological membranes [1], colloids in polymer solution [2], Markov chains in statistics [3], microfluidic devices [4], traffic flow [5], and molecules in zeolites [6], which are treated in the present paper.

Zeolites are complex, crystalline inorganic materials, which have well-defined microporous structure. The zeolite structure is built from corner sharing TO_4 (T=Si, P, Al, Ga, etc.) tetrahedral units, which are linked together to form a more or less complex but precisely repetitive framework of interconnecting cavities and channel structures of nanometric or subnanometric dimensions. These void interior spaces can accommodate guest molecules such as water and cations (usually metallic), which compensate for the charge deficit due to the aluminum/silicon substitution. Their high internal surface, internal acidity, and thermal stability are some of the unique properties that make them an important class of catalytic materials for petrochemical and industrial processes. Besides, these materials are used as molecular sieves, ion exchangers, and adsorbents. Among our past research interests, we considered two zeolites, bikitaite [7] and Li-ABW [8], both showing parallel straight channels, where hydrogen-bonded linear chains of water molecules run along the axis of the channels, parallel to regular rows of lithium ions sticking to the channel surface. A pictorial view of these structures is represented in Fig. 1.

Classical molecular dynamics (MD) simulations at high temperature (800–900 K) extended to the nanosecond scale were performed on these systems. While the full hydrated systems did not show any diffusion, because the molecules cannot pass each other in the channels due to a high energy barrier, when some molecules are removed diffusion occurs according to the single-file mechanism, as water molecules do not diffuse between different channels. In Refs. [7,8] the diffusive process was studied by evaluating the mean square displacement (MSD) along the channel axis, the diffusion coefficient at infinitely low concentration (one molecule per channel), the potential energy acting on the water molecules along the channels, which is approximately sinusoidal for both zeolites, and the related energy barriers, which are different (19 kJ/mol for bikitaite and 13 kJ/mol for Li-ABW). In this work we intend to extend these analyses. In particular, we compare the results of our simulations with the predictions of anomalous diffusion theory modeled by using fractional diffusion equations. At high coverage, the agreement is reasonably good. At low coverage, interesting phenomena appear in the simulation results, such as multimodal propagators, which could be interpreted on the basis of fractional Fokker-Planck equation. The results are discussed also in view of different theories that have been proposed to model the single-file diffusion process.

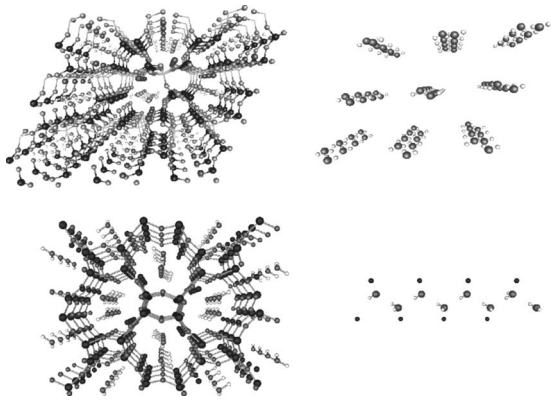

FIG. 1. Top: the structure of bikitaite (left) as seen from the b axis and its water molecules chains (right). Bottom: the structure of Li-ABW as seen from the c axis (left) and a side view of one water molecule chain (right). Symbols of the elements: small white spheres: H; Small black spheres: Li; medium gray spheres: O; large dark gray spheres: Al and Si.

*Electronic address: pino@uniss.it

II. THEORETICAL AND SIMULATED PROPAGATORS

A. Theory

The milestones of the phenomenological theory of diffusion in homogeneous media are well known [9]. In 1855 Adolf Fick proposed the following equation to represent the diffusion process by:

$$\frac{\partial}{\partial t}c(\mathbf{r},t) = D\nabla^2 c(\mathbf{r},t), \tag{1}$$

where $c(\mathbf{r},t)$ is the concentration of the diffusing species at the position $\mathbf{r}$ and time t, and D is the diffusion coefficient, which is constant (at constant temperature).

Fick's law was reinterpreted in 1905 by Einstein, who derived it from statistical mechanics principles by supposing that the fluid-diffusing particles move independently from each other under the effect of the thermal agitation. From this new viewpoint, the concentration in a position $\mathbf{r}$ at a given time, $c(\mathbf{r},t)$, becomes proportional to the probability $W(\mathbf{r},t)$ of finding a particle in the same position and at the same time. $W(\mathbf{r},t)$ is known also as a *propagator*.

It can be shown that the time evolution of $W(\mathbf{r},t)$ is determined by Eq. (1), and for a particle initially in the origin of a d-dimensional space a is given by

$$W(\mathbf{r},t) = \frac{1}{(4\pi Dt)^{d/2}}\exp\left(-\frac{r^2}{4Dt}\right). \tag{2}$$

Thus the mean square displacement (MSD) of the particle for a d-dimensional space is

$$\langle r^2(t)\rangle = \int r^2 W(\mathbf{r},t)d^d r = 2dDt. \tag{3}$$

The distribution (2) can be derived from a "random walk" model of the diffusion, that is, by supposing that every particle is moved so that a "step" of length a in any direction always requires on average the same time.

In various complex systems, diffusion processes no longer follow Gaussian statistics, Fick's law fails to describe the transport behavior, and one finds:

$$\langle r^2(t)\rangle \propto t^{\alpha}, \tag{4}$$

with $\alpha \neq 1$.

A consistent mathematical generalization of the Fick's equation for $\alpha \neq 1$ can be derived by considering the "continuous-time random walk (CTRW)" model [10]. This model is based on the idea that the length of a given step a, as well as the waiting time τ elapsing between two successive steps, are drawn from continuous distributions. It is important to remark that this derivation is obtained, as evidenced by Balakrishnan [11], by taking the limits of the step length $a \to 0$ and simultaneously of the mean jump rate $\lambda \to \infty$.

In order to model the single-file diffusion, one can consider the theory of anomalous diffusion for a system of particles subject to a constant friction flowing in a *one-dimensional* space. According to the CTRW scheme, the diffusive process should be described, as a first approximation, by the equation

$$\frac{\partial}{\partial t}W(r,t) = {}_0D_t^{1-\alpha}K_\alpha \nabla^2 W(r,t), \tag{5}$$

where r is the coordinate along the axis, ${}_0D_t^{1-\mathrm{A}}$ is the Riemann-Liouville operator or fractional derivative of order $1-\alpha$ defined by

$${}_0D_t^{1-\alpha}W(r,t) = \frac{1}{\Gamma(\alpha)}\frac{\partial}{\partial t}\int_0^t dt' \frac{W(r,t')}{(t-t')^{1-\alpha}}, \tag{6}$$

and K_α is a generalized diffusion constant, which is related to MSD by

$$\langle r^2(t)\rangle = \frac{2K_\alpha}{\Gamma(1-\alpha)}t^{\alpha}, \tag{7}$$

which has the same time dependence as Eq. (4). For single-file diffusion it was found by Harris [12] on the basis of statistical considerations that the asymptotic value of α for long times is $\alpha = \frac{1}{2}$. This result was confirmed using different routes or proofs, among others, by Arratia [3], Levitt [13], Kärger [14], van Beijeren *et al.* [15], and Kollmann [16].

The general solution of Eq. (5) in one-dimensional space for $\alpha = \frac{1}{2}$ can be evaluated from a series expansion [10]

$$W(r,t) = \frac{1}{\sqrt{4K_{1/2}t^{1/2}}}\sum_{n=0}^{\infty}\frac{(-1)^n}{n!\Gamma(1-(1/2)[n+1]/2)}\left(\frac{r^2}{K_{1/2}t^{1/2}}\right)^{n/2}. \tag{8}$$

The theoretical predictions for anomalous diffusion of particles subject to a potential energy, besides a constant friction, can be computed from the fractional Fokker-Planck (FP) equation [10,17], which still is derived within a CTRW scheme,

$$\frac{\partial}{\partial t}W(r,t) = {}_0D_t^{1-\alpha}\tilde{L}_{FP}W(r,t), \tag{9}$$

with

$$\tilde{L}_{FP} = \frac{\partial}{\partial r}\frac{V'(r)}{m\eta_\alpha} + K_\alpha\frac{\partial^2}{\partial r^2}, \tag{10}$$

where m is the mass of the particle, $V'(r) = [V(r)]/k_B T$ (k_B being the Boltzmann constant and T the temperature), η_α is the generalized friction constant, and K_α is the generalized diffusion coefficient, the same as in Eq. (5). As reported in Refs. [7,8], the potential energy acting on the water molecules along the channels, adsorbed in both simulated zeolites, is approximately sinusoidal.

If the FP operator is solved by the method of separation of the variables [10,17,18], one obtains an eigenequation of $\tilde{L}_{FP}$, which, for a sinusoidal potential, can be transformed into the Mathieu equation [19]

$$\frac{\partial^2\psi}{\partial r^2} + [a - 2q\cos(2r)]\psi = 0. \tag{11}$$

Unfortunately, the solutions of Eq. (11), known as Mathieu functions, cannot be calculated in closed form nor as simple series expansion, although an attempt was recently proposed [20]. Recently, for the solutions of fractional FP

equation with a periodical potential some asymptotic properties were derived [21] and a numerical algorithm for evaluating explicitly the solutions was reported [22].

However, we preferred to leave both series expansions and numerical solutions for future work and to consider an approximation whose analytical solutions are known. Indeed, as the potential energy around the minimum can be approximated by a harmonic potential and at high coverage the allowed excursion of the molecules does not exceed one period of the potential, we attempted to apply the fractional derivative treatment of single-file diffusion for particles subject to a harmonic potential [10,23], using the following exact expansion, valid for $\alpha=\frac{1}{2}$:

$$W(r,t) = \sqrt{\frac{k_{el}}{2\pi k_B T}} \sum_{n=0}^{\infty} \frac{1}{2^n n!} E_{1/2}\left[-n\left(\frac{t}{\tau}\right)^{1/2}\right] \times H_n\left(r'\sqrt{\frac{k_{el}}{2k_B T}}\right) H_n\left(r\sqrt{\frac{k_{el}}{2k_B T}}\right) \exp\left(-\frac{k_{el} r^2}{2k_B T}\right), \tag{12}$$

where $E_\alpha(z)=\Sigma_{n=0}^{\infty} z^n/\Gamma(1+n\alpha)$ is the Mittag-Leffler function, which for $\alpha=\frac{1}{2}$ is equal to [10]

$$E_{1/2}(-z) = \mathrm{erfc}(z)\exp(z^2), \tag{13}$$

so that the final expansion reads

$$W(r,t) = \sqrt{\frac{k_{el}}{2\pi k_B T}} \sum_{n=0}^{\infty} \frac{1}{2^n n!} \mathrm{erfc}\left[n\left(\frac{t}{\tau}\right)^{1/2}\right] \times \exp\left(n^2 \frac{t}{\tau}\right) H_n\left(r'\sqrt{\frac{k_{el}}{2k_B T}}\right) H_n\left(r\sqrt{\frac{k_{el}}{2k_B T}}\right) \times \exp\left(-\frac{k_{el} r^2}{2k_B T}\right). \tag{14}$$

In Eqs. (12) and (14), $k_{el}=m\omega^2$ is the elastic constant for the harmonic oscillator, k_B is the Boltzmann constant, T is temperature, H_n are Hermite polynomials of order n, r' is the initial coordinate (in our cases $r'=0$), and τ is a time constant defined by [10],

$$\tau^{-1/2} = \frac{\omega^2}{\eta_{1/2}} = \frac{m\omega^2}{m\eta_{1/2}} = \frac{k_{el}}{m\eta_{1/2}}, \tag{15}$$

where $\eta_{1/2}$ is a generalized friction constant, the same as in Eq. (10), which is related to the generalized diffusion coefficient $K_{1/2}$ by the following equation [10]:

$$K_{1/2} = \frac{k_B T}{m\eta_{1/2}}, \tag{16}$$

so that τ can be derived using only universal constants and parameters evaluated from the simulated systems by comparing Eqs. (15) and (16),

$$\tau = \left(\frac{k_B T}{k_{el} K_{1/2}}\right)^2. \tag{17}$$

The general solutions of fractional diffusion equation [Eq. (5)] and fractional FP equation [Eq. (9)], namely Eqs. (8) and (12), respectively, can be applied to specific cases by considering their boundary conditions, which are multifarious [15,24,25]. For instance, the system may be finite or infinite, with a finite number of particles but unlimited, periodic or not, and the initial momentum may be zero or finite. In the cases considered in this work, the initial momentum of the simulated systems was zero and they were subject to periodic boundary conditions, so that the number of molecules per file was constant and they behaved as if they could not leave the simulation box, corresponding to a boundary condition of two adsorbing walls at $r=\pm L/2=a$ (L being the length of the simulation box), which is given by

$$W(-a,t) = W(a,t) = 0. \tag{18}$$

In order to find the propagator subject to these boundary conditions to be compared with the one derived from the simulations, one could apply the method of images [24,26,27] to Eq. (5), but, as suggested in Ref. [18], one can solve the equivalent fractional derivative Fokker-Planck equation with a "box" potential (zero inside the box, infinite outside). The solution is reported in Ref. [18] and is given by

$$W(r,t) = \sum_{n=1}^{\infty} \frac{2\sin[\lambda_n(r_0+a)]\sin[\lambda_n(r+a)]}{2a} E_{1/2}[-\lambda_n^2 K_{1/2} t^\alpha], \tag{19}$$

where $\lambda_n=n\pi/2a$ and $E_{1/2}(z)$ is the Mittag-Leffler function, which for $\alpha=1/2$ is defined in Eq. (13).

Theoretical predictions about single-file diffusion have been derived also independently of the CTRW scheme. Lebowitz and Percus [28] obtained the exact solution for the propagator for an infinite one-dimensional system of hard rods. In the long-time limit, the propagator reduces to a Gaussian as given by Eq. (2) with a suitable value of the diffusion coefficient, so that apparently no anomalous diffusion should follow. However, Levitt [13] has described a generalization of this process in which the one-dimensional dynamics was combined with randomized background. Again, the exact solution for the propagator was obtained. The most interesting result of this analysis is that, under rather general conditions, the long-time limit of $W(r,t)$ is given by

$$W(r,t) = \frac{\sqrt{\rho}}{2(\pi D_0 t)^{1/4}} \exp\{-\rho r^2[\pi/(16 D_0 t)]^{1/2}\}, \tag{20}$$

where D_0 is the diffusion coefficient the particle would have if it were the only particle in the infinite one-dimensional system and ρ is the density of the point particles. If rods of length ℓ are used, one gets the same result by using $\rho=\rho'/(1-\rho'\ell)$, where ρ' is the density of the rods. By evaluating the second moment of $W(r,t)$ from Eq. (20),

$$\langle r^2(t)\rangle = \int dr' r'^2 W(r',t), \tag{21}$$

one gets the MSD,

$$\langle r^2(t)\rangle = 2\frac{1-\rho'\ell}{\rho'}\sqrt{\frac{D}{\pi}}t^{1/2} = 2Ft^{1/2}, \tag{22}$$

where $F=(1-\rho'\ell/\rho'\sqrt{D/\pi})$ is the single-file mobility factor. Equations (20)–(22) have been derived in different ways by using probabilistic approaches [14–16], yielding also the *small* and *large* time limits of the propagator and of MSDs depending on the boundary conditions. In particular, these limits have been derived by assuming normal diffusion, or Gaussian propagator [Eq. (2)], in the time interval between the collisions of the particles and by applying the special constraints arising from the excluded mutual passage. For intermediate times, one approximate estimate of the time dependence of MSD was reported [15], but the corresponding propagator was not derived explicitly. Within this approach, an interesting method claimed as suitable for calculating exact propagators (in the long-time limit) in single-file systems of different nature and subject to different constraints was proposed by Rödenbeck *et al.* [24]. It is based on the reflection principle and yields propagators for a general class of systems, as shown by numerical examples and by the derivation of the asymptotic behavior of an infinite channel [Eq. (21)].

Using the method of images, the propagator subject to the boundary conditions given by Eq. (18), $Q(r,t)$ is obtained from a general propagator [such as those reported in Eqs. (12) and (20)] or from the solution of an unconstrained diffusion equation [such as Eqs. (5) or (9)] by

$$Q(r,t) = \sum_{n=-\infty}^{\infty} [W(r+4na,t) - W(-r+4na+2a,t)], \tag{23}$$

where it is supposed that the particle is confined in the interval $]-a,a[$ and that the initial position is $r=0$.

It is essential, while considering the theoretical modeling of single-file discussion, to remark that the same dependence of MSDs on $t^{1/2}$ is found *irrespective of the form of the propagator used among those reported in* Eqs. (8), (12), (14), (19), and (20), i.e., the second moments of all these propagators, evaluated through Eq. (21), are proportional to $t^{1/2}$, provided that no drift due to initial conditions and/or biased applied potential is present. Obviously, as the propagators are different, moments of order higher than 2 will show a different trend.

The differences in the propagators are also related to different assumptions and approximations used to develop the different theoretical models from which they are derived and, in turn, to the physics of the single-file diffusion. This phenomenon is seemingly simple, but its interpretation in terms of mathematical models is unexpectedly complex, essentially because of the presence of strong correlations in the particle motion. Let us consider a system of particles diffusing on the same line and suppose that they cannot pass one another. Zero total momentum can be assumed without loss of generality, because collective motions of the system can be superimposed easily to the zero-momentum single-file diffusion. As long as the particles are not in contact, they move, independently of each other, under the action of random forces of zero average and white spectrum, as those caused by a thermal bath. A potential may be also present along the line, provided that its energy barriers are thermally accessible, so that diffusion is permitted. Interactions between particles are assumed of repulsive nature (smooth or hard core). Attractive forces may be present, but they must not be so strong to cause the particles to stick together.

From the viewpoint of a tagged particle, its excursion is determined by the positions of the adjacent particles on both sides, whose average distance depends on the particle density or coverage. In order to find the probability of larger and larger excursions, if the constraint of constant density is applied, the position of more and more neighbor particles are to be considered, because they must squeeze together. In the limit of infinite excursion, all the particles, except the tagged one, are close packed. The density of probability of a given excursion r, which is just the value of the propagator $W(r,t)$ in r at some time t, can be related to the density of probability of the class of configurations of the whole system compatible with such excursion at time t. This is more evident for finite or periodic systems, where the maximum excursion is bounded. Moreover, if a potential acts on the particles, the positions corresponding to the minima of the potential will be more frequently visited, so that maxima or shoulders corresponding to these positions will appear in the propagator, superimposed to its trend derived in absence of the potential. The time evolution of the excursion depends obviously on the time evolution of the position of the neighboring particles, which in turn is related to the previous history of their neighbors, more and more back in time as more and more large excursions are considered. In this respect, the single-file diffusive process is essentially non-Markovian. Moreover, the diffusive single-file motion will be, on average, slower than in the case of normal diffusion, because in the latter case, for the same dynamical conditions, there is a finite probability that the tagged molecule will pass an adjacent one and move farther than under single-file conditions.

A mathematically convenient assumption to derive a theory of single-file diffusion is to model it in terms of random walk, by considering steps beginning and finishing with collisions between particles and applying the constraint of single-file motion; that is, the space ordering of the particles must remain unchanged. If one assumes that the steps are all equal to their average value and that between collisions the average motion follows a Gaussian propagator [Eq. (2) in one dimension], a more or less involved statistical reasoning [3,12–16,24,28] leads to an average MSD described by Eq. (22) and to an asymptotic propagator represented by Eq. (20). Obviously, this approximation does not consider the details of the distributions of the step length and of their duration, and thus it is especially suitable in the long time limit.

On the contrary, in the CTRW scheme [10,11] the step length and their duration are assumed to be variable, according to explicit probability densities. The propagator is then evaluated from a master equation relating the probability density to reach a given position at a certain time to the same previous ones. In the continuum limit, the master equation becomes an integral equation. If a special analytical form is assumed for the waiting time distribution $\psi(t)$ (giving the

probability density for the time interval t between two consecutive steps), namely,

$$\psi(t) = \frac{1}{\Gamma(\alpha)} \frac{1}{(t)^{1+\alpha}}, \tag{24}$$

in which α assumes values in the range $0 < \alpha < 1$, the integral equation can be interpreted in terms of fractional diffusion equation, once the condition of the conservation of the flux of the particles is imposed [11]. It is to be remarked that fractional diffusion equation was derived to cope with anomalous diffusion in general and not explicitly with single-file diffusion, but it is used to model this kind of diffusion on the basis of the resulting correct trend of MSD versus time, given by Eq. (7). It is beyond the scope of this paper to treat the various forms of the equivalent fractional differential equation (fractional with respect to time, space, or both) and of the integral equation from which they are derived. The above details about the most popular theoretical models of single-file diffusion were reported in view of the comparison with experimental and simulation results.

When two ore more theoretical models of a given phenomenon are competing, the common practice of scientific work it to turn to possibly crucial experiments. Unfortunately, experimental studies of single-file diffusion are rare and, at our best knowledge, the propagator derived from experimental data was reported in two cases only [29,30]. In the former case the propagator was evaluated for a single-file system developed by confining polystyrene colloidal spheres in one-dimensional circular channels of micrometer scale in aqueous suspension. In order to prevent colloidal particles from sticking together, the spheres were doped with Fe_2O_3 clusters and were paramagnetic so that, when an external magnetic field was applied perpendicular to the sample plane, a magnetic dipole was induced in the colloids that gave rise to a repulsive pair interaction potential. The diffusion was ensured by Brownian motion. Optical video microscopy pictures were digitalized and the instantaneous particle coordinates were extracted and saved in a computer for later analysis. From the obtained trajectories the MSDs were derived, which followed the predicted $t^{1/2}$ behavior for more than two decades of time after an initial steeper trend. More importantly for our discussion, the propagator was evaluated at different times and an excellent fit of Eq. (20) was obtained. Further data on the same system were later reported [31], confirming the $t^{1/2}$ behavior, but the focus was on the evaluation of the static structure factor and of the related collective diffusion coefficient. In the latter study reporting the propagator derived from experimental data [30], a system consisting of silica colloid spheres was suspended in water and confined in straight and narrow grooves. The grooves were printed on a polydimethylsiloxane substrate and their width was sufficiently small to prevent the spheres from passing one other. The propagator was assumed to have the Gaussian form

$$W(r,t) = \frac{1}{(2\pi\langle r^2(t)\rangle)^{1/2}} \exp[-r^2(t)/2\langle r^2(t)\rangle], \tag{25}$$

which is compatible with any dependence of $\langle r^2(t)\rangle$ on t. In other words, Eq. (25) includes Eqs. (2) and (20) as special cases. The fitting of experimental data to Eq. (25) was good. The MSDs were proportional to t at short times, changed smoothly to $\langle r^2(t)\rangle \propto t^{\alpha} (\alpha < 1)$ at later time, and reached $\langle r^2(t)\rangle \propto t^{1/2}$ at long time for the higher concentrations.

Other experimental studies on single diffusion of molecules in zeolites of one-dimensional channel structure [32], of aqueous and polymer solutions of negatively charged silica particles in straight polymer channels [33], and of millimetric charged balls in a circular channel [34], all confirmed the $\langle r^2(t)\rangle \propto t^{1/2}$ behavior at long times but did not report the propagator. We note in passing that the system considered by Coupier *et al.* [34], having a small number of particles, $N=12$, and periodic conditions, was very similar to those simulated in the present work, and indeed also the reported MSD shows a trend similar to those found in this work. Seemingly, the scarce experimental data would be in favor of a propagator represented by Eq. (20), at least at long times, but the comparison with different predicted propagators was not considered.

B. Comparison between simulated and theoretical propagators

Computer simulations of single-file systems date back at least from a paper by Richards [35], where a Monte Carlo (MC) evaluation of some correlation functions and of the MSD of a system containing 4000 particles is reported. It is shown that the single-particle MSD follows the expected dependence on time, $\langle r^2(t)\rangle \propto t^{1/2}$, but no propagator was derived. Extended MC simulations of different systems with various number of particles, coverage, and boundary conditions, including the hard reflecting walls reported by van Beijeren *et al.* [15], all confirmed the results of previous simulations and theoretical predictions. Further MC simula-

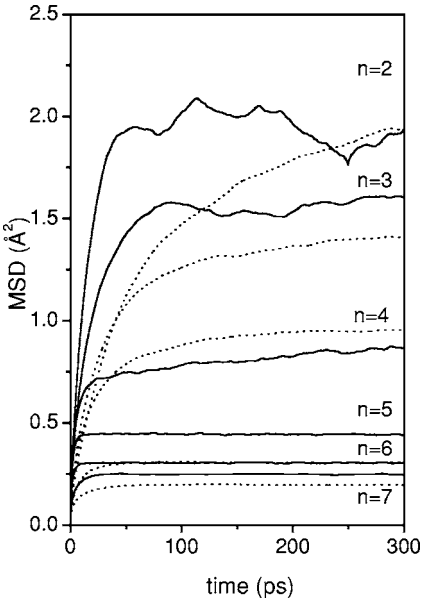

FIG. 2. Mean square displacements (MSDs) of water molecules for different number of molecules per channel (n) computed with respect to the center of mass of the molecules contained in each channel. The relative occupancy θ is given by $n/8$. Solid lines: Li-ABW at about 750 K; dotted lines: bikitaite at about 900 K.

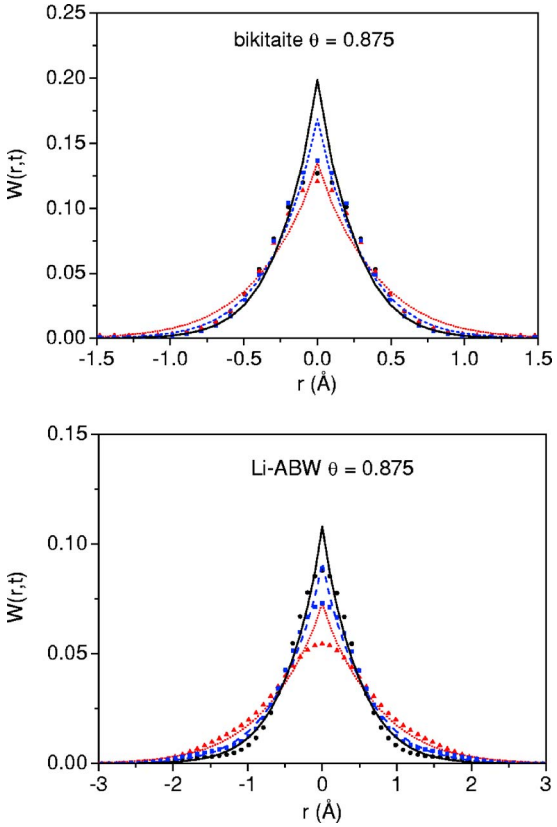

FIG. 3. (Color online) Propagators evaluated from MD simulations (symbols) and from Eq. (19) (lines) at three different times (short times) for relative occupancy $\theta=0.875$ of bikitaite (top) and Li-ABW (bottom). Circles (solid lines), squares (dashed lines), and triangles (dotted lines) correspond to increasing times at which the propagators are evaluated from the simulations (theoretical models). The same meaning applies to Figs. 4, 7–10, 13, and 14.

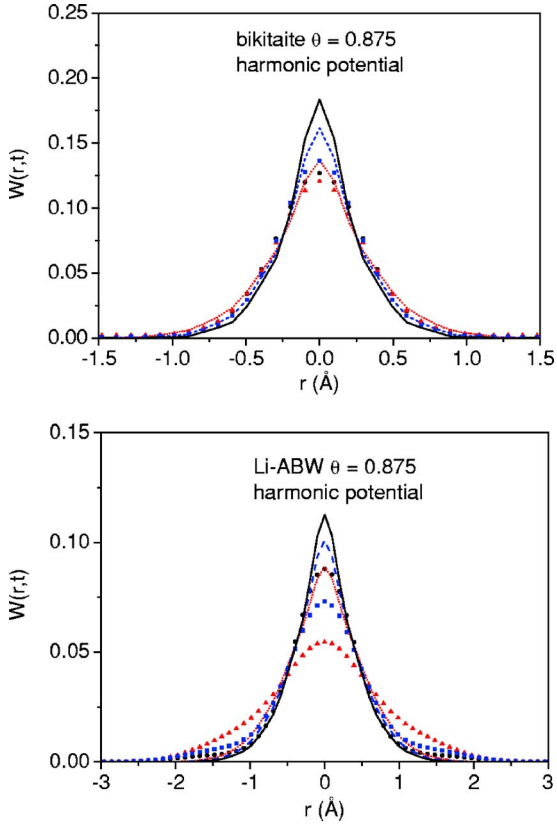

FIG. 4. (Color online) Propagators evaluated from MD simulations (symbols) and from Eq. (14) (lines) at three different times (short times) for relative occupancy $\theta=0.875$ of bikitaite (top) and Li-ABW (bottom).

tions were performed in various systems and boundary conditions [36,37], or using special techniques such as Smart Monte Carlo [38], but, to our best knowledge, the propagators were evaluated only by Rödenbeck *et al.* [24] to verify the non-Gaussian behavior of the "exact propagators" predicted for some boundary conditions, and by Heinsalu *et al.* [22], who used a MC scheme for the numerical integration of fractional FP equations with a potential $U(r)=V(r)-Fr$, where $V(r)=V(r+L)$ is a periodic substrate potential and F is an external static force ("washboard potential"). Literature provides only a few examples of MD simulations in single-file systems. Hahn *et al.* [32,39] studied molecular diffusion in zeolites of one-dimensional channel structure and confirmed the experimental trend $\langle r^2(t)\rangle \propto t^{1/2}$. The obtained mobility factors compared well with the measured values [32]. It was also shown in detail that for periodic systems with conserved total momentum zero for sufficiently long times, the MSD will approach a finite value, which must be markedly smaller than the period of the file length [39]. This phenomenon was further analyzed by Pal *et al.* [40], who obtained for model systems results similar to ours [7,8]. Mon and Percus [41] proposed a simplified model to simulate the anomalous self-diffusion in a single-file fluid under the influence of random background forces. Most recently, Taloni and Marchesoni [42] reported extended simulations of single-file systems of particles diffusing on a one-dimensional periodic substrate both for noiseless (ballistic) and stochastic dynamics. The dependence of the corresponding diffusion coefficients on the density and temperature of the particles was determined and analytically interpreted within the formalism of standard Brownian motion. Once again it was confirmed that some general features of single-file diffusion process as, for instance, the dependence of MSDs on time, are independent of the potential form. Both MD (for relatively short times) and dynamic MC (for longer times) were used by Vasenkov *et al.* [43] to study single-file molecular transport near the channel boundaries in a finite channel, finding MSDs approaching a constant value for sufficiently long channels. None of these MD simulation studies reported the propagators.

In our previous studies, simulations of water adsorbed in two zeolites, biktaite [7], and Li-ABW [8] at the nanosecond scale were performed using classical MD at high temperature (800–900 K). As shown in Fig. 1 and anticipated in the Introduction, these zeolites contain parallel straight channels, where hydrogen-bonded linear chains of water molecules run along the axis of the channels, parallel to regular rows of lithium ions sticking to the channel surface. The simulation box had in both cases sides of approximately 2 nm. For bikitaite it contained 864 atoms of the aluminosilicate framework (including 72 Li cations) forming nine channels and

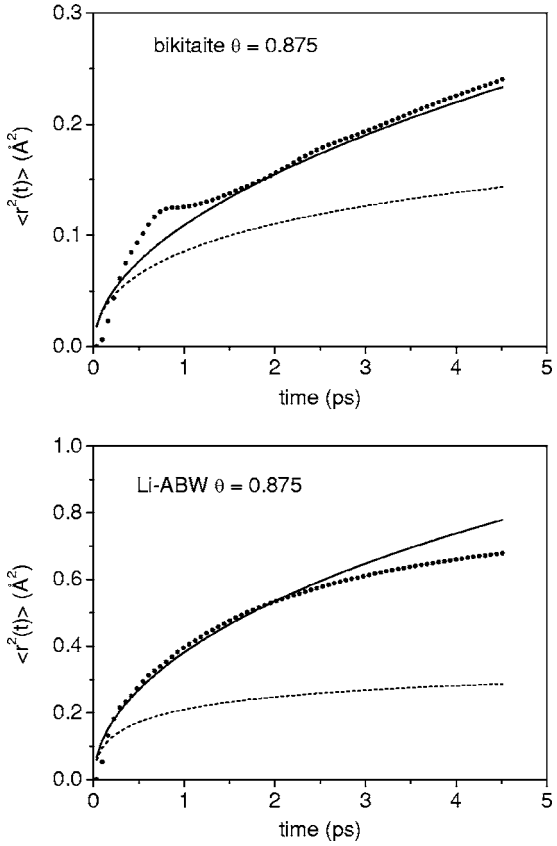

FIG. 5. MSDs of water molecules along the channel axis (short times) evaluated from MD simulations (symbols) and using the propagator computed from Eq. (19) (solid lines) and from Eq. (14) (dashed lines) for relative occupancy θ=0.875 of bikitaite (top) and Li-ABW (bottom). In Eq. (19) $\alpha=\frac{1}{2}$.

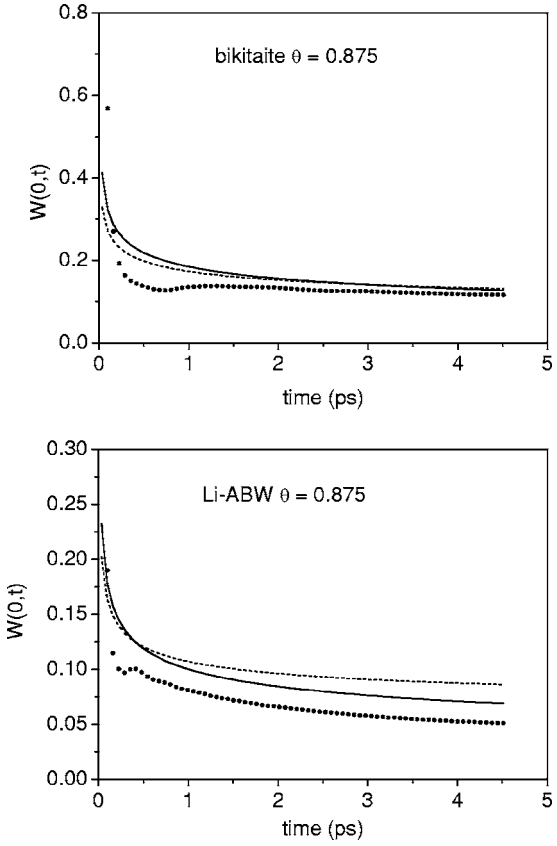

FIG. 6. Propagators as a function of time (short times) at r=0 evaluated from MD simulations (symbols) and computed from Eq. (19) (solid lines) and from Eq. (14) (dashed lines) for relative occupancy θ=0.875 of bikitaite (top) and Li-ABW (bottom).

contained up to eight water molecules per channel. For Li-ABW the aluminosilicate framework atoms (including 64 Li cations) were 448 and formed eight channels containing as well up to eight water molecules each.

All atoms, including the aluminosilicate framework acting as an efficient heat bath for the adsorbed molecules, were allowed to move without constraint under the action of empirical potentials developed in our laboratory [8,44] while a sophisticated electric field-dependent model for flexible water was adopted [45]. Structural and vibrational properties computed using our model agree well with the experiment. Even at high temperature (750 K), no diffusion of water was detected, indicating that, at least with the adopted model, the energy barrier for water molecules to pass each other with full loading is much higher than k_BT, and indeed it was evaluated as 84 kJ/mol for bikitaite and 56 kJ/mol for Li-ABW. In order to explain the experimentally observed dehydration process, it may be suggested that, after heating, in real (finite) crystals, water can escape from the free ends of the channels, inducing a defect-driven stepwise diffusion, which eventually leads to dehydration. Therefore, to elucidate the diffusive mechanism, partially dehydrated zeolites in bikitaite and Li-ABW was simulated at high temperatures, ranging from 400 K to 1000 K for all possible water content (1–8 molecules per channel).

MSDs evaluated with respect to the centre of mass of the molecules adsorbed in each channel (so that the total momentum is zero, see Ref. [7]), are depicted in Fig. 2 and behave as expected for single-file systems with periodic boundary conditions and initial zero total momentum [40,43]. The position of a water molecule was represented by the coordinates of its oxygen atom. At sufficiently short times, of the order of 0.2 ps, which are not visible in Fig. 2 but are evidenced in logarithmic scale, the MSDs are proportional to t^2 (ballistic or free motion). Then, depending on temperature and coverage, the single-file regime sets in and the exponent of time in Eq. (4) should gradually become $\alpha=\frac{1}{2}$. Indeed, this is true (within a few percent) for the simulated systems, in spite of the characteristics of the molecules (they are not spherical although in fast rotational motion) and of the channels (they are not smooth, and along the channel axis the molecules are subject to a potential energy approximately sinusoidal with a period very close to the effective molecular diameter, 2.4 Å, with energy barriers of 19 kJ/mol for bikitaite and 13 kJ/mol for Li-ABW). After times ranging from a few to 100 ps, depending again on temperature and coverage, the MSDs reach a maximum and begin to oscillate around a constant value. As shown by Hahn and Kärger [39], the approximate maximum value of MSDs under the above mentioned boundary conditions as a function of the coverage can be predicted, and the compari-

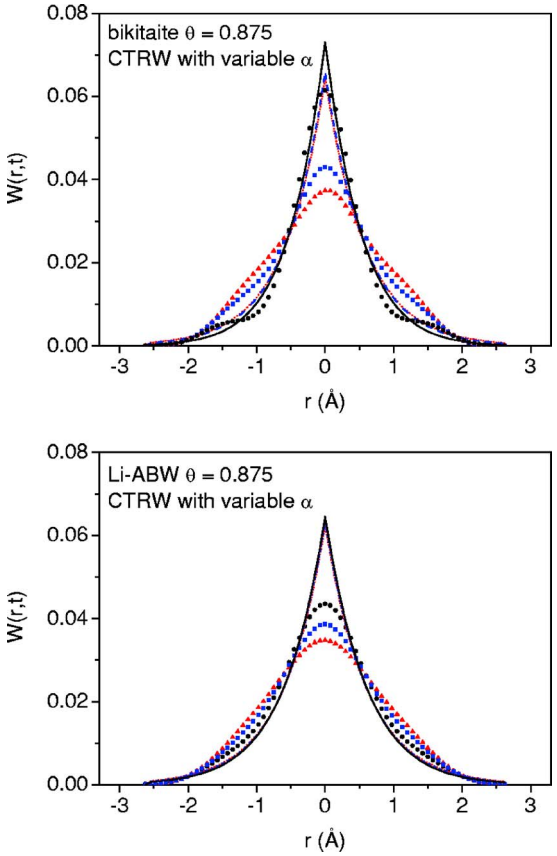

FIG. 7. (Color online) Propagators evaluated from MD simulations (symbols) and from Eq. (19) (lines) at three different times (long times) for relative occupancy θ=0.875 of bikitaite (top) and Li-ABW (bottom). The value of α appearing in Eq. (19) is obtained as a function of time from the simulations using Eq. (7).

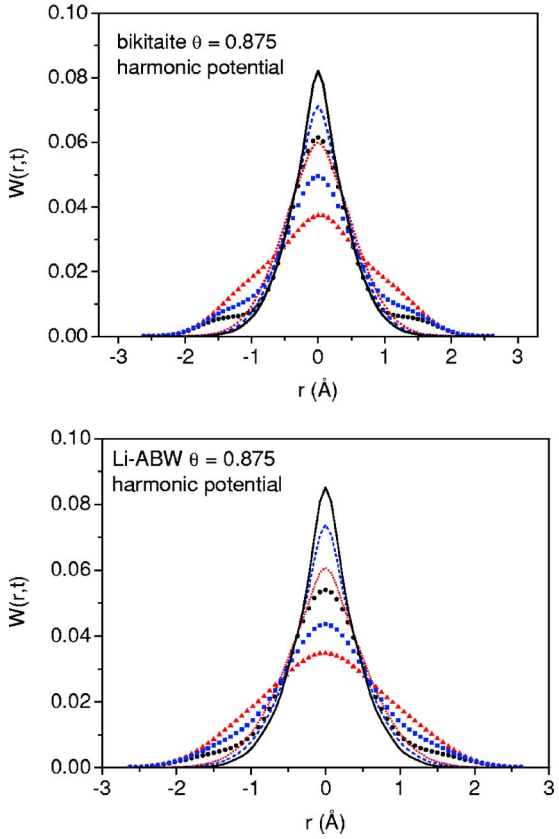

FIG. 8. (Color online) Propagators evaluated from MD simulations (symbols) and from Eq. (12) (lines) at three different times (long times) for relative occupancy θ=0.875 of bikitaite (top) and Li-ABW (bottom). The value of α appearing in Eq. (12) is obtained as a function of time from the simulations using Eq. (7).

son with the simulations results is reasonable [7,8].

In order to compare the theory and the simulated results, we evaluate the propagators directly from MD simulations, as the frequencies of finding the coordinate of a molecule (with respect to the center of mass of the chain to which it belongs) in given time and space intervals Δt and Δr, respectively, within two kinds of time ranges:

(i) time ranges for which, in each simulation, the MSDs remain proportional to $t^{1/2}$ with $\alpha=\frac{1}{2}$ (within error bounds of a few percent) (short times);

(ii) time ranges extended until the MSDs approach the constant value (long times), in which α assumes different values in the range $0<\alpha<1$.

The space ranges corresponded to the maximum elongation reached at the end of the time ranges. A grid of 71×71 time and space intervals was found as a good compromise to get sufficiently smooth and symmetric distributions without missing interesting details. The theoretical propagators were evaluated for short time ranges from Eq. (19) directly, using Eq. (13) to evaluate the Mittag-Leffler function, or from Eqs. (14) by applying the method of images [Eq. (23)] in order to obey the constraint given by Eq. (18). For long times, the Mittag-Leffler function in Eqs. (12) and (19) was derived using the general procedure reported in Ref. [22] and the propagators were evaluated also from Eq. (20) and from the procedure proposed in Ref. [24], applying the method of images when needed.

The parameters contained in the theoretical propagator equations were obtained from the simulations. In particular, the value of $K_{1/2}$ in Eqs. (17) and (19) was derived by fitting the simulated MSDs using Eq. (7). As for the parameters appearing in Eq. (14), the elastic constant for the harmonic oscillator: $k_{el}=m\omega^2$ was evaluated by fitting the potential energy of the simulated systems around a minimum and the time constant τ was obtained from Eq. (17). No adjusting of these parameters to reproduce the simulated propagators was attempted. The diffusion coefficient at infinite dilution D_0 in Eq. (20) was derived from simulations with one molecule per channel [7,8].

In general, the agreement is good only for the highest values of the relative occupancy. For lower occupancies the maximum excursion for a molecule exceeds one molecular diameter and the effects of the potential energy along the channel appear as resulting in a multimodal propagator (see below). However, the agreement is still good on average, so that the MSDs evaluated from Eq. (7) reproduce well the MSDs resulting from the simulations. In Fig. 3 examples of the propagators evaluated from the simulations for the maximum simulated relative occupancy $\theta=7/8=0.875$ of bikitaite and Li-ABW are displayed together with the corresponding theoretical ones computed from Eq. (19) at three

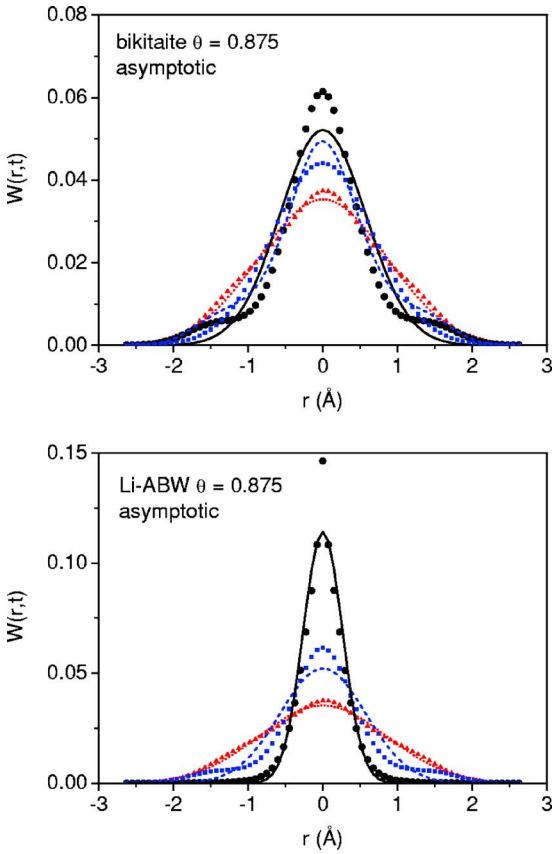

FIG. 9. (Color online) Propagators evaluated from MD simulations (symbols) and from Eq. (20) (lines) at three different times (long times) for relative occupancy θ=0.875 of bikitaite (top) and Li-ABW (bottom).

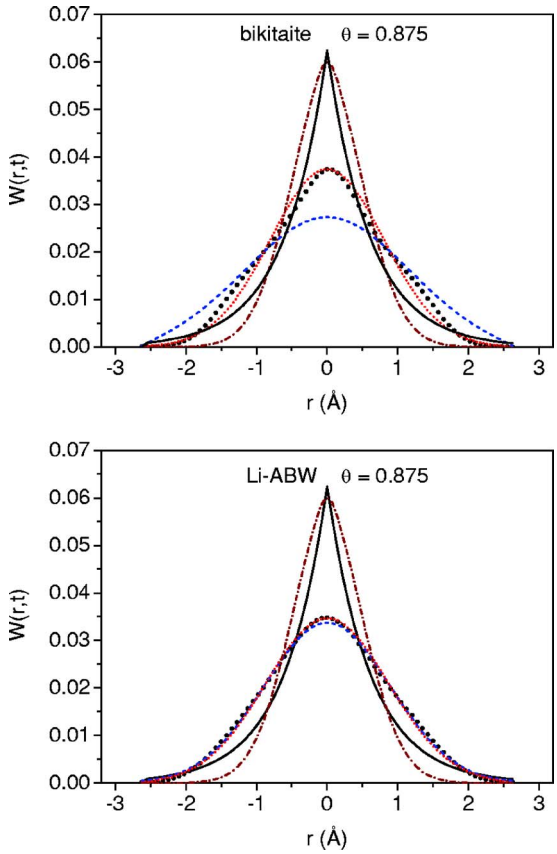

FIG. 10. (Color online) Propagators evaluated from MD simulations (symbols) and from Eq. (19) (solid line), from Eq. (12) (dash-dotted line), from Eq. (20) (dotted line), and from the procedure reported in Ref. [24], using corrected values of the diffusion coefficient at infinite dilution (dashed line), at the longest times for which simulation results are available (see text) for relative occupancy θ=0.875 of bikitaite (top) and Li-ABW (bottom).

different times. In order to ensure a good convergence at short times, 4000 terms were included in the summation. Interestingly, although the summation in Eq. (19) involves functions which are continuous on the whole $]-a,a[$ interval, around $r=0$ the propagator shows a trend very close to the cusp, which should be a typical feature for subdiffusive ($\alpha<1$) processes according to the fractional diffusion equation derived according to the CTRW scheme [10]. However, the cusp does not appear in the simulated propagator. Nevertheless, the overall fit appears good. In Fig. 4 the propagators evaluated from the simulations, always for relative occupancy θ=0.875, are compared with the corresponding theoretical ones computed from Eq. (14). In this case the cusp is not present in the theoretical propagator, but they are too narrow for both systems, as would be expected, because of assuming confining potentials narrower than those derived from the simulations. Theoretical and simulated behaviors of $\langle r^2(t)\rangle$ are reported in Fig. 5. They were derived from the propagators by evaluating their second moments according to Eq. (21) and, as for propagators, the agreement is better for single-file diffusion without potential energy acting on the diffusing particles [Eq. (19)]. Finally, the trend of the propagators as a function of time (at $r=0$), $W(0,t)$, resulting from theory and simulations, is reported in Fig. 6, and the same remark as for the MSDs holds.

In Figs. 3–6 the results are reported for time intervals in which the $t^{1/2}$ behavior is closely followed by the simulated MSDs (short times). For a comparison at longer times, we derived the propagator for the whole time interval in which $0<\alpha<1$ using *instantaneous* values of α and K_α fitted to the simulated MSDs via Eq. (7). As remarked above, at long times also Eq. (20) and the procedure proposed in Ref. [24] to obtain the long-time limit of the "exact propagators" can come into play, and we evaluated these propagators too. However, while the MSDs obtained at long times for Eqs. (12), (19), and (20) were reasonable, the propagator obtained from the "exact propagator" procedure was too wide if the values of D_0 derived from the simulations were used. Nevertheless, these values were adjusted in order to fit the simulated propagators at the longest time available. In particular, for bikitaite (Li-ABW) the fitting value was D_0 $=4.0\ 10^{-11}\mathrm{m}^2\ \mathrm{s}^{-1}$ ($D_0=5.0\ 10^{-10}\ \mathrm{m}^2\ \mathrm{s}^{-1}$), that is 72.5 (20) times smaller than the same parameter derived from the simulations, yielding an excellent fit. It is important to remark that the procedure proposed in Ref. [24] does not involve the time explicitly. It includes the Gaussian distribution and its integrals in which the squared variance is assumed to be $\langle r^2(t)\rangle=2D_0t$ but, as the propagator is given, at least for the case of interest, without dependence on time, in the Gaussian distribution and its integrals the form used in

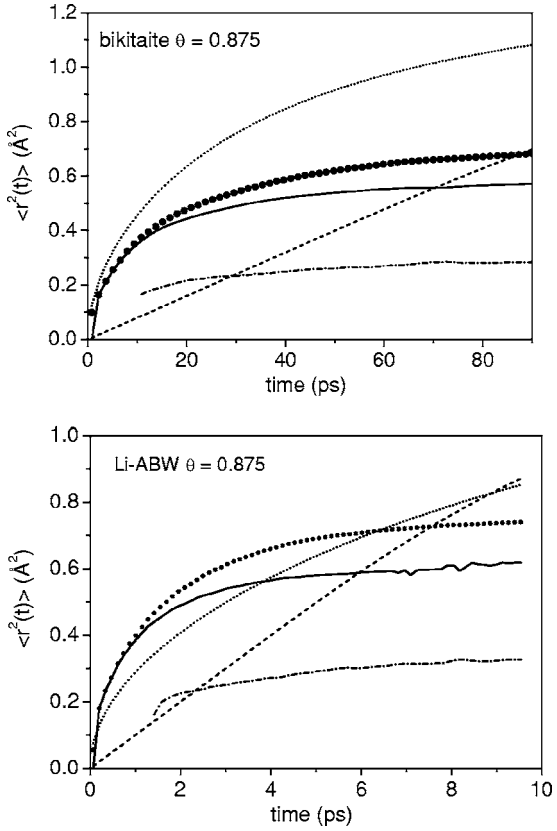

FIG. 11. MSDs of water molecules along the channel axis (long times) evaluated from MD simulations (symbols) and using the propagators computed from Eq. (19) (solid lines), from Eq. (12) (dash-dotted line), from Eq. (20) (dotted line), and from the procedure reported in Ref. [24], for relative occupancy $\theta=0.875$ of bikitaite (top) and Li-ABW (bottom).

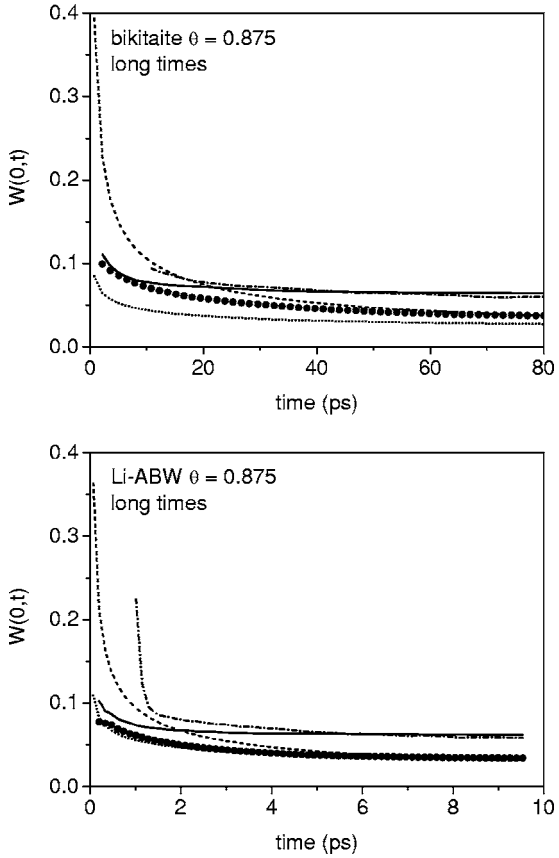

FIG. 12. Propagators as a function of time (long times) at $r=0$ evaluated from MD simulations (symbols) and computed from Eq. (19) (solid lines), from Eq. (12) (dash-dotted line), from Eq. (20) (dotted line), and from the procedure reported in Ref. [24], for relative occupancy $\theta=0.875$ of bikitaite (top) and Li-ABW (bottom).

Eq. (25) should be preferred. For the systems considered in this work, $\langle r^2(t)\rangle$ becomes constant at sufficiently long times, so that the modified values of D_0 are just those which yield the long-time limit of $\langle r^2(t)\rangle$. In the case of Eq. (20), using values of D_0 derived from the simulations, an excellent fit resulted for Li-ABW but for bikitaite propagator was slightly too wide although still reasonable. In Figs. 9–14 the results are reported for the longest time intervals for which the MSDs are increasing before reaching the first maximum. They will be discussed in the next section.

The behavior of the simulated propagator at low relative occupancies shows an interesting multimodal trend, which is due to the presence of a periodical potential along the channel axis. Some examples are reported in Figs. 7 and 8. It is worth noting that some of the secondary maxima of the propagators evaluated for bikitaite for Li-ABW become shoulders because the energy barrier to diffusion is lower than for bikitaite [8]. Indeed, at low temperature the maxima are present also for Li-ABW. Multimodal propagators were recently reported as solutions of fractional FP for the "washboard potential" (see above) [22] as well as with a symmetric, quartic well $U(r)\propto r^4$ *without minima* [46,47]. In the latter case, it was shown [48] that maxima in the propagator arise from changes in *curvature* and not from potential minima and this is confirmed in our simulations. Despite the presence of maxima or shoulders in the propagators, the MSDs are smooth with a dependence on time similar to that of the unimodal propagators, at it appears in Fig. 2.

III. DISCUSSION

The comparison of the propagators evaluated from the simulation results with those predicted by different theoretical models, which are collected in Figs. 3–14 gives rise to a series of points to be discussed in detail. As it appears in Figs. 3, 9, and 10, a cusp at $r=0$ is present in the propagators derived from the CTRW theory, Eq. (5) and evaluated using Eq. (19), irrespective of the value of α. This cusp is neither visible in the propagators obtained from the simulations nor from experiments [29,30] and is probably an artifact arising, as above remarked and evidenced by Balakrishnan [11], by taking the limits of the CTRW step length $a\rightarrow 0$ and simultaneously of the mean jump rate $\lambda\rightarrow\infty$. However, in real and simulated systems, the step length is finite and can be long, as at finite coverage the particles cover a finite space before colliding with an adjacent one and between two collisions the diffusive motion is "normal." We evaluated the average jump length and time for bikitaite (1.36 Å and 2.08 ps) and

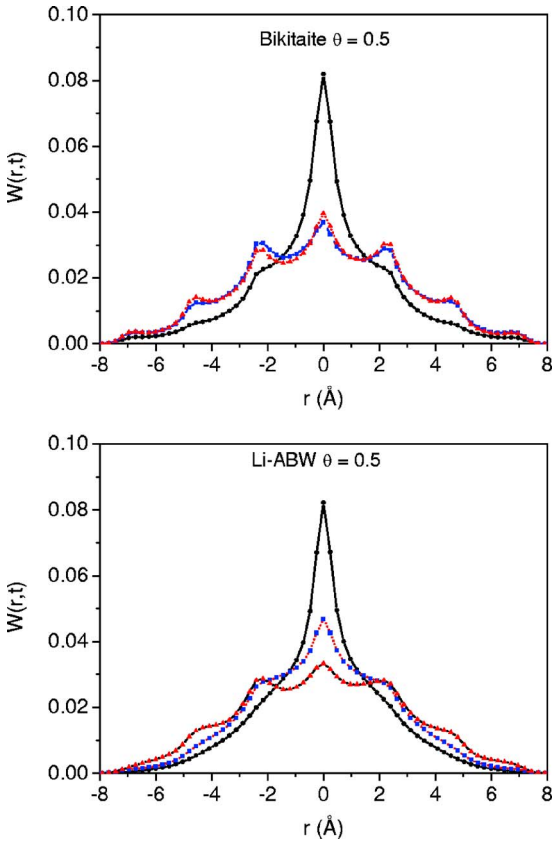

FIG. 13. (Color online) Propagators evaluated from MD simulations at three different times for relative occupancy θ=0.5 of bikitaite (top) and Li-ABW (bottom).

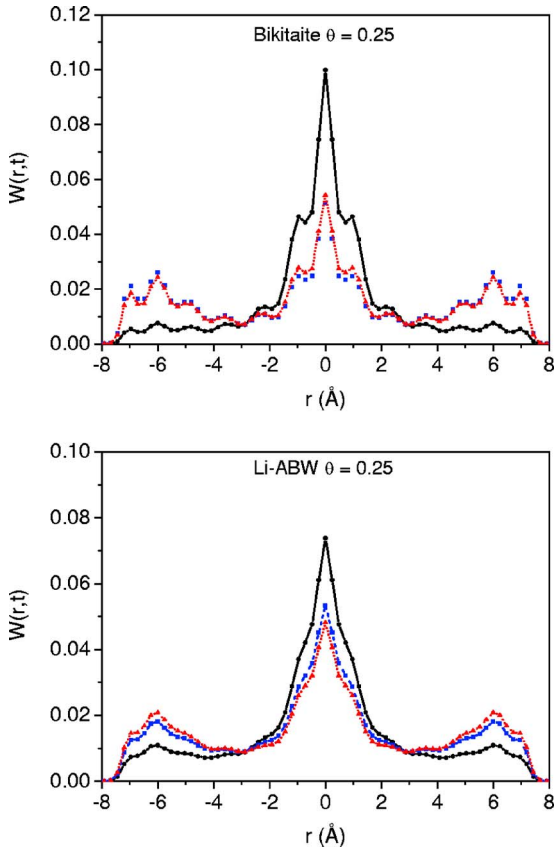

FIG. 14. (Color online) Propagators evaluated from MD simulations at three different times for relative occupancy θ=0.25 of bikitaite (top) and Li-ABW (bottom).

for Li-ABW (0.36 Å and 0.96 ps). These values are not negligible with respect to the space and time scales of the simulations. Another trend of this kind of propagators, which does not fit simulation or experimental results, is the long r behavior at long times (see Figs. 9 and 10). Besides the evident differences visible in the figures, the asymptotic behavior reported in Eq. (45) of Ref. [24], which is valid for large elongations, does not agree with the trend of Eq. (20). Nevertheless, the propagators derived from fractional diffusion equations, as shown in Figs. 5 and 11, yield the best fit of the MSDs at any considered time, at least by using the instantaneous values of α derived from the simulations for longer times. The propagator derived from the fractional FP equation with harmonic potential through Eq. (14), for $\alpha=\frac{1}{2}$, or Eq. (12), for $\alpha\neq\frac{1}{2}$, after application of the method of images [Eq. (23)], is always more or less too narrow (see Figs. 4, 8, and 10), as expected, because the harmonic potential is more confining than the real potential. However, the cusp at $r=0$ is less peaked than in the case of fractional diffusion equation with constant potential. The dependence on time of the propagators stemming from CTRW theory at $r=0$, $W(0,t)$ is close to that shown by the simulated propagators at short times but less satisfactory at longer times (see Figs. 6 and 12, respectively). At long times, the asymptotic propagator given by Eq. (20), to which the method of images was applied, fits well the simulated propagators (see Figs. 9 and 10), but it is not able to reproduce the trend of MSDs, which remain proportional to $t^{1/2}$, whereas in the simulations α vanishes at long times. On the contrary, the behavior of $W(0,t)$ reported in Fig. 13 is reasonable at long times. In Figs. 10 and 11, it is shown that the "exact propagator" obtained using the procedure proposed in Ref. [24], as remarked in the previous section, at the longest times fits well the ones derived from simulations only after a correction of the MSDs but the dependence of MSDs on time is not correct, as it expect from its functional form. However, the trend of $W(0,t)$ shown in Fig. 12 is in agreement with the simulations.

Taking into account all these considerations, the point that naturally arises is about the most suitable theoretical scheme to model the single-file diffusion.

In the studies using the probabilistic approach here considered [3,12–16,24], apart from the use of the normal diffusion equation as a starting point, no general equation whose solution yields directly the propagator of single-file diffusion is proposed. However, in most of them, the asymptotic (long-time) form of the propagator is derived, which fits well both experimental and simulation results. For intermediate times only, Laplace-transformed propagators for different boundary conditions were proposed [15], but for no real time and space approximation was worked out, and they were used to evaluate (correct) trends of $\langle r^2(t)\rangle$, but, as it was shown above, this is not a crucial test.

On the other hand, a fractional diffusion equation (or fractional FP equation if a potential acts on the diffusing par-

ticles), as illustrated for instance in Ref. [10] and intended as a way to model anomalous diffusion, yields the correct time dependence of MSD on time, namely time raised to a power equal to the fractional order of the equation α, and as shown in this work, the corresponding propagator can reproduce some peculiar features of the simulation and of experimental results. The failure to represent the behavior around $r=0$ can be easily explained (see above) and accepted as a consequence of the approximations assumed to derive the diffusion equation. The problem appears harder if the behavior at long times and large r is considered, also because the comparison with simulations or experiments is less easy. Moreover, as we already remarked, the value of α can depend on time, according to the features of the system (which can be finite, infinite, periodic, open, bounded, etc.), but a general way to derive the time dependence of α, as far as we know, is still lacking. In this view, in our opinion, an interesting approach is that proposed by Gorenflo *et al.* [49], who approximate the CTRW connected with fractional diffusion equation by means of a variety of models of random walks, discrete in space and time. One of the cases they consider is discrete random walk models for the non-Markovian fractional diffusion, in which the probabilities of sojourn at a given point in a given instant depend on the *whole history* of the particle. If we correctly understood this approach, some of these models, which depend just on the value of α, could correspond to the single-file diffusion under different conditions (systems which are finite, infinite, periodic, open, bounded, etc.), and a general equations for the single-file diffusion including the prediction of the time dependence of α on the boundary conditions could be derived. Fractional diffusion equations of distributed order (depending on different values of α have been recently proposed [50], which can be the starting point for future developments of the single-file diffusion theory.

ACKNOWLEDGMENTS

We are grateful to J. Klafter, F. Mainardi, F. Marchesoni, A. Taloni, and A. V. Chechkin for useful discussions and for encouraging this work. This research is supported by the Italian Ministero dell'Istruzione, dell'Università, e della Ricerca (MIUR) (Italy), by the COSMOLAB Consortium (CYBERSAR Supercomputing Research Project), by Università degli studi di Sassari, and by Istituto Nazionale per la Scienza e Tecnologia dei Materiali (INSTM).

[1] F. Gambale, M. Bregante, F. Stragapede, and A. M. Cantu, J. Membr. Biol. **154**, 69 (1996).
[2] C.-Y. Chou, B. C. Eng, and M. Robert, J. Chem. Phys. **124**, 044902 (2006).
[3] R. Arratia, Ann. Probab. **11**, 362 (1983).
[4] A. D. Stroock, M. Weck, D. T. Chiu, W. T. S. Huck, P. J. A. Kenis, R. F. Ismagilov, and G. M. Whitesides, Phys. Rev. Lett. **84**, 3314 (2000).
[5] H. Y. Lee, H. W. Lee, and D. Kim, Phys. Rev. Lett. **81**, 1130 (1998).
[6] J. Kärger and D. M. Ruthven, *Diffusion in Zeolites and Other Microporous Solids* (Wiley-Interscience, New York, 1992).
[7] P. Demontis, G. Stara, and G. B. Suffritti, J. Chem. Phys. **120**, 9233 (2004).
[8] P. Demontis, G. Stara, and G. B. Suffritti, Microporous Mesoporous Mater. **86**, 166 (2005).
[9] A. Fick, Philos. Mag. **10**, 30 (1855). **10**, 30 (1855); A. Fick, Ann. Phys. Chem. **94**, 59 (1855); A. Einstein, Ann. Phys. **17**, 549 (1905); J. Crank, *The Mathematics of Diffusion* (Clarendon Press, Oxford, 1970).
[10] R. Metzler and J. Klafter, Phys. Rep. **339**, 1 (2000).
[11] V. Balakrishnan, Physica A **132**, 569 (1985); R. Gorenflo, F. Mainardi, D. Moretti, and P. Paradisi, Nonlinear Dyn. **29**, 129 (2002); F. Mainardi, A. Vivoli, and R. Gorenflo, Fluct. Noise Lett. **5**, L291 (2005).
[12] T. E. Harris, J. Appl. Probab. **2**, 323 (1965).
[13] D. G. Levitt, Phys. Rev. A **8**, 3050 (1973).
[14] J. Kärger, Phys. Rev. A **45**, 4173 (1992).
[15] H. van Beijeren, K. W. Kehr, and R. Kutner, Phys. Rev. B **28**, 5711 (1983).
[16] M. Kollmann, Phys. Rev. Lett. **90**, 180602 (2003).
[17] E. Barkai, Phys. Rev. E **63**, 046118 (2001).
[18] Kwok Sau Fa and E. K. Lenzi, Phys. Rev. E **72**, 011107 (2005).
[19] M. Abramowitz and I. A. Stegun, Eds. *Handbook of Mathematical Functions* (Dover Pub. Inc., New York, 1972).
[20] D. Frenkel and R. Portugal, J. Phys. A **34**, 3541 (2001).
[21] I. Goychuk, E. Heinsalu, M. Patriarca, G. Schmid, and P. Hänggi, Phys. Rev. E **73**, 020101(R) (2006).
[22] E. Heinsalu, M. Patriarca, I. Goychuk, G. Schmid, and P. Hänggi, Phys. Rev. E **73**, 046133 (2006).
[23] R. Metzler, E. Barkai, and J. Klafter, Phys. Rev. Lett. **82**, 3563 (1999).
[24] C. Rödenbeck, J. Kärger, and K. Hahn, Phys. Rev. E **57**, 4382 (1998).
[25] J. M. D. MacElroy and S.-H. Suh, J. Chem. Phys. **106**, 8595 (1997).
[26] W. Feller, *An Introduction to Probability Theory and Its Applications*, Vol. 2 (Wiley, New York, 1971).
[27] A. Compte, Phys. Rev. E **55**, 6821 (1997).
[28] J. L. Lebowitz and J. K. Percus, Phys. Rev. **155**, 122 (1967).
[29] Q.-H Wei, C. Bechinger, and P. Leiderer, Science **287**, 625 (2000).
[30] B. Lin, M. Meron, B. Cui, S. A. Rice, and H. Diamant, Phys. Rev. Lett. **94**, 216001 (2005).
[31] C. Lutz, M. Kollmann, and C. Bechinger, Phys. Rev. Lett. **93**, 026001 (2004).
[32] K. Hahn, J. Kärger, and V. Kukla, Phys. Rev. Lett. **76**, 2762 (1996).
[33] C.-Y. Chou, B. C. Eng, and M. Robert, J. Chem. Phys. **124**, 044902 (2006).
[34] G. Coupier, M. Saint Jean, and C. Guthmann, Phys. Rev. E **73**, 031112 (2006).
[35] P. M. Richards, Phys. Rev. B **16**, 1393 (1977).

[36] J. Kärger, M. Petzold, H. Pfeifer, S. Ernst, and J. Weitkamp, J. Catal. **136**, 283 (1992).
[37] K. K. Mon and J. K. Percus, J. Chem. Phys. **117**, 2289 (2002).
[38] D. S. Sholl and K. A. Fichthorn, J. Chem. Phys. **107**, 4384 (1997); K. Hahn and J. Kärger, *ibid.* **109**, 5691 (1998); D. S. Sholl and K. A. Fichthorn, *ibid.* **109**, 5693 (1998).
[39] K. Hahn and J. Kärger, J. Chem. Phys. **100**, 316 (1996).
[40] S. Pal, G. Srinivas, S. Bhattacharyya, and B. Bagchi, J. Chem. Phys. **116**, 5941 (2002).
[41] K. K. Mon and J. K. Percus, J. Chem. Phys. **119**, 3343 (2003).
[42] A. Taloni and F. Marchesoni, Phys. Rev. Lett. **96**, 020601 (2006).
[43] S. Vasenkov, A. Shüring, and S. Fritzsche, Langmuir **22**, 5728 (2006).
[44] P. Demontis, G. Stara, and G. B. Suffritti, J. Phys. Chem. B **107**, 4426 (2003).
[45] P. Demontis, S. Spanu, and G. B. Suffritti, J. Chem. Phys. **112**, 8267 (2001).
[46] A. Chechkin, V. Gonchar, J. Klafter, R. Metzler, and L. Tanatarov, Chem. Phys. **284**, 233 (2002).
[47] A. V. Chechkin, J. Klafter, V. Yu. Gonchar, R. Metzler, and L. V. Tanatarov, Phys. Rev. E **67**, 010102(R) (2003).
[48] A. V. Chechkin, V. Yu. Gonchar, J. Klafter, R. Metzler, and L. V. Tanatarov, J. Stat. Phys. **115**, 1505 (2004).
[49] B. Gorenflo, G. De Fabritiis, and F. Mainardi, Physica A **269**, 78 (1999); B. Gorenflo, F. Mainardi, D. Moretti, G. Pagnini, and P. Paradisi, *ibid.* **305**, 106 (2002); B. Gorenflo, F. Mainardi, D. Moretti, G. Pagnini, and P. Paradisi, Chem. Phys. **284**, 521 (2002).
[50] A. V. Chechkin, R. Gorenflo, and I. M. Sokolov, Phys. Rev. E **66**, 046129 (2002); I. M. Sokolov, A. V. Chechkin, and J. Klafter, Acta Phys. Pol. B **35**, 1323 (2004).